

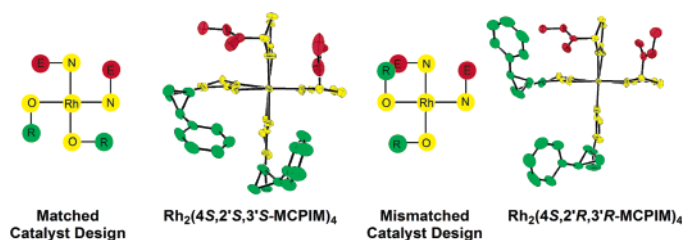
“Matched/Mismatched” Diastereomeric Dirhodium(II) Carboxamidate Catalyst Pairs. Structure–Selectivity Correlations in Diazo Decomposition and Hetero-Diels–Alder Reactions

Michael P. Doyle,^{*,†} John P. Morgan,[†] James C. Fettinger,[†] Peter Y. Zavalij,[†] John T. Colyer,[‡] Daren J. Timmons,[‡] and Michael D. Carducci[‡]

Department of Chemistry and Biochemistry, The University of Maryland, College Park, Maryland 20742, and Department of Chemistry, University of Arizona, Tucson, Arizona 85721

mdoyle3@umd.edu

Received March 29, 2005



Homo-ligated dirhodium(II) carboxamidates provide well-defined structural frameworks with which to investigate catalyst-controlled multiple asymmetric induction (“match/mismatch” effects). Diastereomeric pairs of methyl 2-oxoimidazolidine-4(*S*)-carboxylate ligands containing 2-phenylcyclopropane (4*S*,2'*S*,3'*S*-HMCPIM and 4*S*,2'*R*,3'*R*-HMCPIM) and *N*-benzenesulfonylproline (4*S*,2'*S*-HBSPIM and 4*S*,2'*R*-HBSPIM) attachments at the 1-*N*-acyl site have been prepared; the resulting (*cis*-2,2)-Rh₂L₄ compounds have been produced in good yields, and the X-ray crystal structure of each dirhodium(II) compound has been obtained. The incorporation of additional stereocenters into the dirhodium(II) ligands leads to recognizable levels of double asymmetric induction for C–H insertion, cyclopropanation, and hetero-Diels–Alder cycloaddition applications. The configurationally “matched” cases provide modest increases in enantioselectivity for intramolecular C–H insertion reactions relative to the model catalyst Rh₂(MPPIM)₄, but applications of the configurationally mismatched catalysts result in significant lowering of enantioselectivity. The Rh₂(BSPIM)₄ catalysts show the highest degree of differential selectivity. Hetero-Diels–Alder reactions show inverse behavior from the configurationally matched and mismatched Rh₂L₄ catalysts to that found in the metal carbene transformations.

Introduction

Delineation of the stereochemical factors that allow a chiral catalyst to influence product configuration remains a central problem in asymmetric catalysis.¹ With catalysts whose ligand(s) have multiple stereogenic elements, configurational and conformational complexities arise that can be transmitted as stereoselectivity in product formation. The ligand’s multiple stereocenters may be situated favorably (“matched”) or unfavorably (“mismatched”) for stereocontrol when the catalyst interacts with a prochiral substrate.² Ultimately, the matched

cases may lead to dramatically larger asymmetric induction in the products, whereas the mismatched cases often result in significantly lower selectivity.³ Notable examples of this double asymmetric induction exist in hydrogenation chemistry, focusing primarily on rhodium or ruthenium with bidentate phosphine ligands containing multiple stereocenters.⁴ In particular, modifications of DIOP,⁵ DuPHOS,⁶ and BINAP⁷ ligands, among others,⁸ have led to improvements in enantiocontrol in the matched cases and reductions in enantiocontrol in the mismatched cases. Similar effects have been reported by

* Corresponding author.

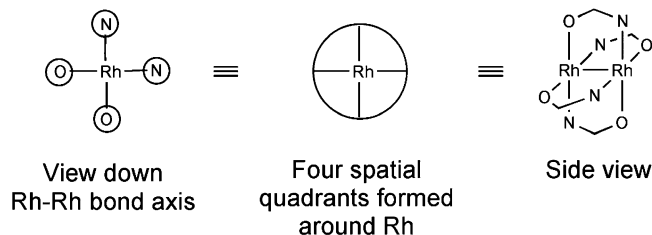
[†] University of Maryland.

[‡] University of Arizona.

(1) (a) Jacobsen, E. N.; Pfaltz, A.; Yamamoto, H. *Comprehensive Asymmetric Catalysis*; Springer: New York, 1999. (b) Vögtle, F.; Stoddart, J. F.; Shibasaki, M. *Stimulating Concepts in Chemistry*; Wiley-VCH: New York, 2000. (c) Williams, J. M. J. *Catalysis in Asymmetric Synthesis*; Sheffield Academic: Sheffield, 1999.

(2) (a) Masamune, S.; Choy, W.; Petersen, J. S.; Sita, L. R. *Angew. Chem., Int. Ed. Engl.* **1985**, *24*, 1–30. (b) Heathcock, C. H.; White, C. T. *J. Am. Chem. Soc.* **1979**, *101*, 7076–7079. (c) Horeau, A.; Kagan, H.-B.; Vigeron, J.-P. *Bull. Soc. Chim. Fr.* **1968**, 3795–3797.

(3) (a) Noyori, R. *Asymmetric Catalysis in Organic Synthesis*; Wiley: New York, 1994. (b) Ojima, I.; Ed. *Catalytic Asymmetric Synthesis*, 2nd ed.; Wiley: New York, 2000. (c) Stephenson, G. R.; Ed. *Advanced Asymmetric Synthesis*; Chapman and Hall: London, 1996.

SCHEME 1. Dirhodium Carboxamidate Complexes in the (*cis*-2,2) Configuration


Katsuki for a broad selection of chemical transformations by the introduction of a binaphthyl unit into the salen ligand.⁹ The strategy employed is the design of multiple stereocenters in the ligand to control the overall catalyst-reactant orientation, which in turn influences product stereochemistry.^{10,11} However, configurational changes in ligands brought about by installing additional chirality are generally unpredictable, and reaction selectivities are determined empirically.⁴

There are no reliable predictive models to explain the structural subtleties of catalysts with multiple chiral centers that lead to dramatic changes in stereoselection, although the “match/mismatch” strategy has been widely applied over the past 20 years.^{1,5–9} Dirhodium(II) carboxamidates offer an appealing framework on which to examine structural influences on reaction stereoselectivity because of their noted structural rigidity and their suitability as catalysts for several chemical transformations.¹² Their construction features four bridging ligands around the dirhodium core so that two nitrogen and two oxygen donor atoms are attached to each rhodium with the composite arranged in a *cis*-2,2 fashion (Scheme 1).¹³ This ligand arrangement affords a relatively inflexible structural framework that is amenable to configurational modifications.

1-Acyl-2-oxo-imidazolidine-4-carboxylates have a framework on which additional stereocenters can be conveniently built.¹⁴ Whereas the configuration of the 4-carboxylate substituent affords enantiomer differentiation,^{12,13} the 1-acyl substituent is known to influence conforma-

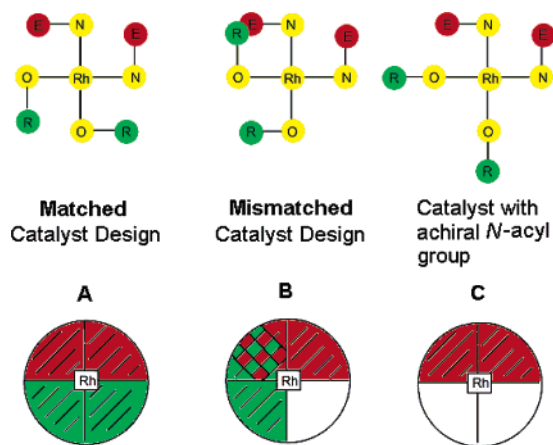
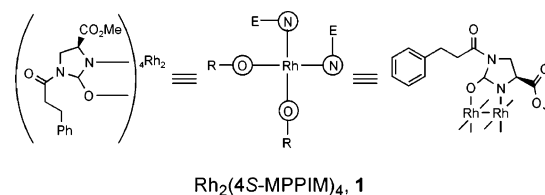


FIGURE 1. Diastereomeric dirhodium carboxamidate complexes depicted with a view along the rhodium–rhodium bond axis.

tional flexibility associated with diastereocontrol.¹⁵ In structures such as $\text{Rh}_2(4\text{S-MPPIM})_4$ (**1**), for example, the



3-phenylpropanoyl group provides optimum structural advantage for control of diastereoselectivity and enantioselectivity in metal carbene carbon–hydrogen insertion reactions^{15,16} and in hetero-Diels–Alder reactions.¹⁷ By introducing chirality into the *N*-acyl substituent, two or more dirhodium(II) carboxamidate diastereoisomers are produced (**A** and **B** in Figure 1) whose configurational orientation is either aligned with (**A**) or opposed to (**B**) that of the 4-carboxylate attachment. In contrast, the achiral *N*-acyl group, as is found in $\text{Rh}_2(4\text{S-MPPIM})_4$, is neither aligned with nor opposed to the configuration of the 4-carboxylate attachment (see **C**). Because the electronic influence of the 1-acyl substituent is expected to be largely invariant with its structure, steric effects on reaction selectivity will govern the outcome. Herein we describe the synthesis of diastereomeric pairs of catalysts based on structural variations in the *N*-acyl substituent, provide X-ray structural analyses that define their match/mismatch relationships, and examine the stereochemical outcomes from their application to metal carbene transformations and Lewis acid catalyzed hetero-Diels–Alder reactions.

(14) Doyle, M. P.; Zhou, Q.-L.; Raab, C. E.; Roos, G. H. P.; Simonsen, S. H.; Lynch, V. *Inorg. Chem.* **1996**, *35*, 6064–6073.

(15) (a) Doyle, M. P.; Kalinin, A. V.; Ene, D. G. *J. Am. Chem. Soc.* **1996**, *118*, 8837–8846. (b) Doyle, M. P.; Tedrow, J. S.; Dyatkin, A. B.; Spaans, C. J.; Ene, D. G. *J. Org. Chem.* **1999**, *64*, 8907–8915. (c) Doyle, M. P.; Davies, S. B.; May, E. J. *J. Org. Chem.* **2001**, *66*, 8112–8119.

(16) (a) Bode, J. W.; Doyle, M. P.; Protopopova, M. N.; Zhou, Q.-L. *J. Org. Chem.* **1996**, *61*, 9146–9155. (b) Doyle, M. P.; Hu, W.; Valenzuela, M. V. *J. Org. Chem.* **2002**, *67*, 2954–2959. (c) Doyle, M. P.; Hu, W. *Chirality* **2002**, *14*, 169–172.

(17) (a) Doyle, M. P.; Phillips, I. M.; Hu, W. H. *J. Am. Chem. Soc.* **2001**, *123*, 5366–5395. (b) Doyle, M. P.; Valenzuela, M.; Huang, P. *Proc. Natl. Acad. Sci. U.S.A.* **2004**, *101*, 5391–5395. (c) Valenzuela, M.; Doyle, M. P.; Hedberg, C.; Hu, W.; Holmstrom, A. *Synlett* **2004**, 2425–2428.

(4) For additional reviews on double asymmetric induction, see: (a) Kolodiazny, O. I. *Tetrahedron* **2003**, *59*, 5953–6018 and references therein. (b) Sharpless, K. B. *Chem. Rev.* **1985**, *25*, 71–77.

(5) (a) Kagan, H.-B.; Dang, T. P. *J. Am. Chem. Soc.* **1972**, *94*, 6429–6433. (b) Kagan, H.-B.; Fiaud, J. C.; Hoornaert, C.; Meyer, D.; Poulin, J. C. *Bull. Soc. Chim. Belg.* **1979**, *88*, 923–931. (c) Li, W.; Zhang, X. *J. Org. Chem.* **2000**, *65*, 5871–5874.

(6) Burk, M. J.; Pizzano, A.; Martin, J. A.; Liable-Sands, L. M.; Rheingold, A. L. *Organometallics* **2000**, *19*, 250–260.

(7) Qiu, L.; Qi, J.; Pai, C.-C.; Chan, S.; Zhou, Z.; Choi, M. C. K.; Chan, A. S. C. *Org. Lett.* **2002**, *4*, 4599–4602.

(8) (a) Komarov, I. V.; Borner, A. *Angew. Chem., Int. Ed.* **2001**, *40*, 1197–1200. (b) Huang, H.; Zheng, Z.; Luo, H.; Bai, C.; Hu, X.; Chen, H. *Org. Lett.* **2003**, *5*, 4137–4139. (c) Hua, Z.; Vassar, V. C.; Ojima, I. *Org. Lett.* **2003**, *5*, 3831–3834.

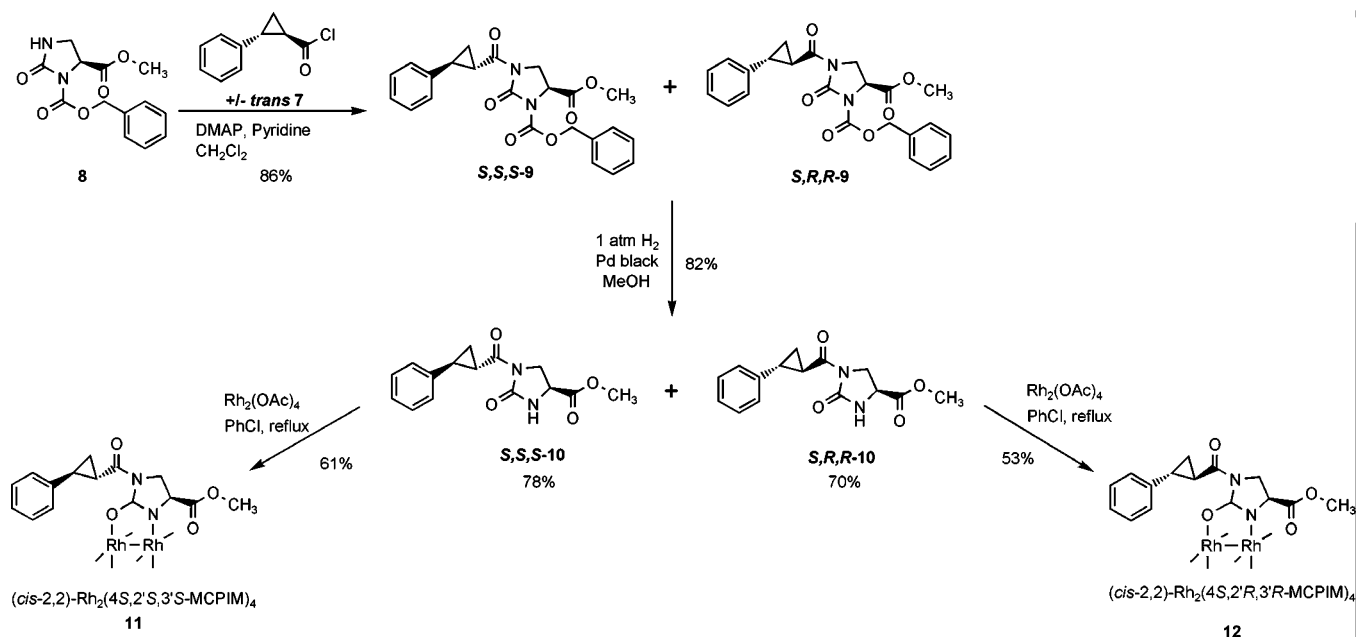
(9) Katsuki, T. *Synlett* **2003**, 281–297.

(10) (a) Huang, H.; Zheng, Z.; Luo, H.; Bai, C.; Hu, X.; Chen, H. *Org. Lett.* **2003**, *5*, 4137–4139. (b) Burgess, K.; Ohlmeyer, M. J.; Whitmire, K. H. *Organometallics* **1992**, *11*, 3588–3600.

(11) For a review of secondary effects in stereoselective catalysis, see: Sawamura, M.; Ito, Y. *Chem. Rev.* **1992**, *92*, 857–871.

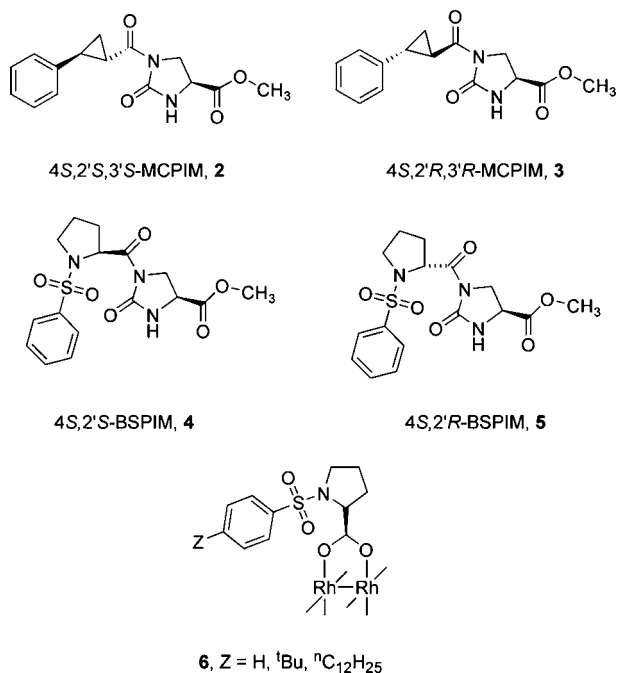
(12) Doyle, M. P.; McKervey, M. A.; Ye, T. *Modern Catalytic Methods for Organic Synthesis with Diazo Compounds*; Wiley: New York, 1998.

(13) (a) Doyle, M. P.; Ren, T. In *Progress in Inorganic Chemistry*; Karlin, K., Ed.; Wiley: New York, 2001; Vol. 49, pp. 113–168. (b) Doyle, M. P. In *Catalysis by Di- and Polynuclear Metal Cluster Complexes*; Adams, R. D., Cotton, F. A., Eds.; VCH Publishers: New York, 1998; Chapter 7.

SCHEME 2. Syntheses of (*cis*-2,2)-Rh₂(4*S*,2'*S*,3'*S*-MCPIM)₄ (11) and (*cis*-2,2)-Rh₂(4*S*,2'*R*,3'*R*-MCPIM)₄ (12)

Results and Discussion

Two sets of diastereomeric dirhodium(II) complexes using the methyl 2-oxo-imidazolidine-4*S*-carboxylate framework were prepared. In ligands **2** and **3**, the *N*-acyl attachment is derived from the enantiomers of *trans*-2-phenylcyclopropanecarboxylic acid, whereas in **4** and **5** the *N*-acyl attachments are prepared from *N*-benzenesulfonylproline enantiomers. The former were employed because of their structural similarity to Rh₂(4*S*-MPPIM)₄ (**1**), whereas the latter have a structural relationship to the chiral dirhodium(II) proline catalysts (**6**) of Davies¹⁸ and McKervery.¹⁹



(*cis*-2,2)-Rh₂(MCPIM)₄. Prior to this work enantiopure *trans*-2-phenylcyclopropanecarboxylic acids had

not been developed on the scale necessary for ligand synthesis. Although highly enantioselective *trans*-selective cyclopropanation of styrene with menthyl diazoacetate is known,²⁰ in our hands this route was inefficient, requiring multiple recrystallizations to ensure high optical purity. On a small scale the *trans*-2-phenylcyclopropanecarboxylic acid racemate was separated by selective recrystallization with brucine,²¹ and chromatographic separation of enantiomers was also achieved. However, the procedure outlined in Scheme 2 was found to be the most effective and practical.

Diastereomeric imidazolidinones **9** were synthesized from **8** and the racemate of *trans*-2-phenylcyclopropanecarboxylic acid chloride (**7**). The product mixture was then used without separation in the subsequent deprotection step to yield **10** as a mixture of diastereomers. Using this optimized route, gram-scale synthesis of both ligand diastereomers was achieved after chromatographic separation [ΔR_f (S,S,S-**10**:S,R,R-**10**) = 0.1, 1:1 hexanes/ethyl acetate]. Dirhodium(II) carboxamidates **11** and **12** were then synthesized through ligand exchange with rhodium(II) acetate and were isolated as red crystals (37% overall yield for Rh₂(4*S*,2'*S*,3'*S*-MCPIM)₄ (**11**); 29% overall for Rh₂(4*S*,2'*R*,3'*R*-MCPIM)₄ (**12**), from acid chloride **7**). The (3,1)-isomers were minor products from these reactions and were not characterized.

Crystal structures for each MCPIM-ligated dirhodium compound are shown in Figures 2 and 3. Selected bond lengths and angles are reported in Tables 1 and 2, respectively. Crystals suitable for X-ray diffraction were obtained by slow evaporation of a solution in methanol with trace acetonitrile (for **11**) or without acetonitrile (for

(18) Davies, H. M. L. *Eur. J. Org. Chem.* **1999**, 2459–2469 and references therein.

(19) Kennedy, M.; McKervery, M. A.; Maguire, A. R.; Roos, G. H. P. *J. Chem. Soc., Chem. Commun.* **1990**, 361–362.

(20) Nishiyama, H.; Itoh, Y.; Matsumoto, H.; Park, S. B. *J. Am. Chem. Soc.* **1994**, *116*, 2223–2224.

(21) The brucine procedure is detailed in Supporting Information: (a) Overberger, C. G.; Shimokawa, Y. *Macromolecules* **1971**, *4*, 718–725. (b) Brückner, C.; Reissig, H. U. *Chem. Ber.* **1987**, *120*, 627–629.

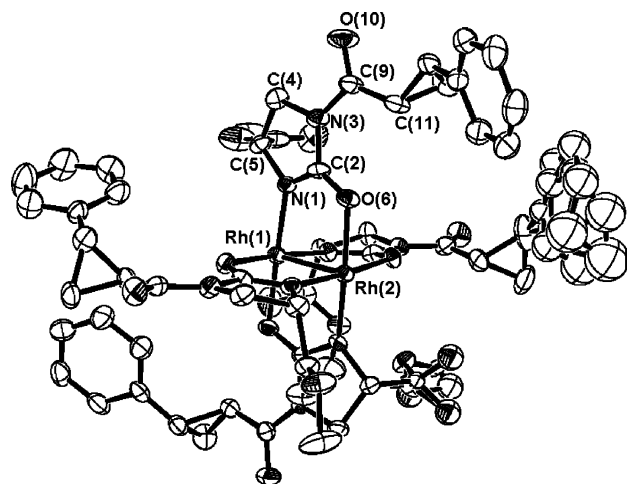


FIGURE 2. ORTEP plot of *(cis-2,2)*-[Rh₂(4*S*,2'*S*,3'*S*-MCPIM)₄-(CH₃OH)(CH₃CN)] (**11**) showing a partial atom labeling scheme. The axial ligands have been removed for clarity. Thermal ellipsoids are scaled to the 50% probability level.

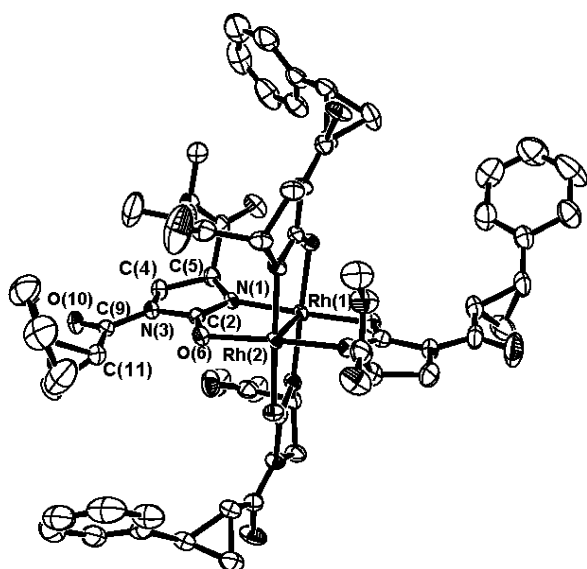
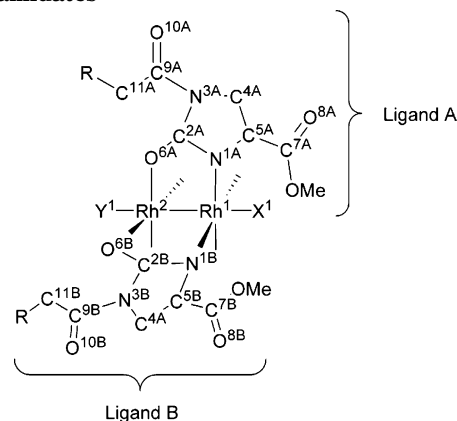


FIGURE 3. ORTEP plot of *(cis-2,2)*-[Rh₂(4*S*,2'*R*,3'*R*-MCPIM)₄-(CH₃OH)₂] (**12**) with a partial atom labeling scheme. The axial ligands have been removed for clarity. Thermal ellipsoids are scaled to the 50% probability level.

12). In both complexes, one of the faces of the cyclopropyl ring in the *N*-acyl group lies over the dirhodium axial site, placing its angular phenyl substituent in one of the spatial quadrants around the bimetallic core.

Viewing the MCPIM catalysts down the rhodium–rhodium bond axis (Figure 4) reveals that these catalysts are indeed configured as shown in Figure 1. Specifically, Rh₂(4*S*,2'*S*,3'*S*-MCPIM)₄ (**11**) has its pendant ester and *N*-acyl side chains oriented in the same direction, forming a counterclockwise spiral. This orientation is particularly well suited to intramolecular reactions in which the active site for reaction is tethered to the dirhodium(II) axial coordination site. Conversely, the ester and *N*-acyl side chains are in configurational opposition in Rh₂(4*S*,2'*R*,3'*R*-MCPIM)₄ (**12**), and this orientation is expected to be a barrier to stereoselectivity enhancement in intramolecular transformations.

TABLE 1. Atom Labels and Selected Bond Lengths (Å) for Imidazolidinone-Ligated Dirhodium(II) Carboxamidates^a



bond	1	11	12	15	16
Rh1–Rh2	2.4637(8)	2.4566(6)	2.4475(4)	2.4394(8)	2.4585(4)
Rh1–N1A	2.012(2)	2.013(5)	2.017(3)	2.022(6)	2.026(4)
Rh1–N1B	2.014(4)	2.016(5)	1.997(3)	1.955(7)	2.014(4)
Rh2–O6A	2.063(2)	2.086(4)	2.059(2)	2.075(5)	2.049(3)
Rh2–O6B	2.055(4)	2.069(4)	2.088(2)	2.068(5)	2.077(3)
Rh1–X1	2.219(4)	2.201(5)	2.291(2)	2.325(5)	2.205(5)
Rh2–Y1	2.202(5)	2.194(5)	2.321(2)	2.325(5)	2.205(5)
N1A–C2A	1.311(4)	1.330(7)	1.311(4)	1.456(9)	1.315(7)
N1B–C2B	1.313(7)	1.305(8)	1.312(4)	1.339(10)	1.298(6)
N1A–C5A	1.463(3)	1.455(7)	1.460(4)	1.305(9)	1.444(6)
N1B–C5B	1.451(7)	1.455(7)	1.461(4)	1.458(10)	1.463(6)
C2A–O6A	1.267(3)	1.262(7)	1.251(4)	1.242(9)	1.265(6)
C2B–O6B	1.271(7)	1.266(7)	1.255(4)	1.244(9)	1.279(6)
C2A–N3A	1.408(3)	1.406(7)	1.426(4)	1.440(9)	1.408(6)
C2B–N3B	1.405(7)	1.420(7)	1.414(4)	1.415(10)	1.415(6)
N3A–C4A	1.454(4)	1.456(8)	1.463(4)	1.461(9)	1.463(6)
N3B–C4B	1.460(7)	1.463(8)	1.468(4)	1.456(11)	1.472(7)
C4A–C5A	1.543(4)	1.554(8)	1.537(5)	1.505(11)	1.566(7)
C4B–C5B	1.551(8)	1.527(8)	1.537(5)	1.490(12)	1.545(7)

^a Data for Rh₂(4*S*-MPPIM)₄ (**1**) are provided for comparison.¹¹ The values in parentheses are the estimated standard deviations and were calculated by $\sigma_{av} = [1/(\sum_i 1/\sigma_i)]^{1/2}$, where σ_i is the estimated standard deviation of each bond length contributing to the average.

(*cis-2,2*)-Rh₂(BSPIM)₄. The synthesis of the diastereomeric BSPIM catalysts is outlined in Scheme 3, focusing on one of the ligand diastereomers. Dirhodium(II) carboxamidates **15** and **16** were prepared by ligand exchange with rhodium(II) acetate [42% overall yield from (*S*)-proline for Rh₂(4*S*,2'*S*-BSPIM)₄ (**15**); 34% overall for Rh₂(4*S*,2'*R*-BSPIM)₄ (**16**) from (*R*)-proline by the same stepwise procedure]. The X-ray crystal structures for the BSPIM pair are shown in Figures 5 and 6. Selected bond lengths and angles are reported in Tables 1 and 2, respectively.

The sterically large prolinyl (*N*-acyl) side chain in the BSPIM structures is twisted nearly perpendicular to the plane of the imidazolidinone ring (C9–C11–C12–C13 dihedral angles = 80–100°). By comparison, the 2-phenylcyclopropyl (*N*-acyl) side chains of **11** and **12** adopt a more extended conformation (C9–C11–C12–C13 dihedral angles = 135–155°), as expected from the rigidity of the cyclopropane ring. Therefore, the pendant phenylsulfonyl groups of **15** and **16** are expected to have a greater influence on the four spatial quadrants surrounding the bimetallic core than do the phenyl substituents of **11** and **12**.

TABLE 2. Selected Bond Angles and Torsion Angles (in deg) for Imidazolidinone-Ligated Dirhodium(II) Carboxamidates^a

bond angle	1	11	12	15	16
Rh2–Rh1–N1A	85.98(5)	85.84(13)	84.17(8)	84.10(17)	84.64(12)
Rh2–Rh1–N1B	86.29(12)	85.24(14)	85.40(8)	86.42(19)	85.72(12)
Rh1–Rh2–O6A	89.45(5)	89.91(11)	91.43(6)	91.66(13)	91.15(10)
Rh1–Rh2–O6B	89.31(10)	89.93(11)	89.57(6)	90.11(14)	89.56(10)
Rh2–Rh1–X1	172.55(7)	177.64(13)	177.18(7)	176.17(14)	174.55(12)
Rh1–Rh2–Y1	171.85(12)	177.73(13)	178.42(7)	176.17(14)	177.26(12)
N1A–Rh1–N1B	92.3(1)	92.06(18)	90.73(11)	91.4(3)	92.18(17)
O6A–Rh2–O6B	90.20(7)	87.56(16)	85.93(9)	88.2(2)	87.50(14)
N1A–Rh1–X1	99.0(1)	93.25(17)	98.44(10)	94.0(2)	92.71(16)
N1B–Rh1–X1	98.3(2)	93.93(17)	95.18(10)	93.4(2)	99.16(17)
O6A–Rh2–Y1	86.4(1)	90.29(17)	86.30(9)	90.97(19)	86.57(15)
O6B–Rh2–Y1	86.0(2)	87.81(17)	90.03(9)	87.25(18)	88.83(16)
Rh1–N1A–C2A	121.3(2)	122.2(4)	121.9(2)	126.4(5)	122.1(3)
Rh1–N1B–C2B	121.0(4)	121.1(4)	122.1(2)	121.3(5)	122.2(3)
Rh1–N1A–C5A	127.9(2)	128.3(4)	128.1(2)	121.9(5)	127.6(4)
Rh1–N1B–C5B	128.1(3)	128.8(4)	126.7(2)	127.2(5)	125.4(3)
Rh2–O6A–C2A	115.9(2)	115.9(4)	113.5(2)	112.5(5)	115.1(3)
Rh2–O6B–C2B	116.6(4)	114.4(4)	114.7(2)	113.9(5)	115.0(3)
N1A–C2A–N3A	111.8(2)	111.8(5)	110.3(3)	110.3(6)	111.6(4)
N1B–C2B–N3B	111.8(5)	111.7(5)	110.7(3)	109.7(7)	111.7(4)
C2A–N3A–C4A	108.7(2)	108.6(5)	108.5(3)	107.7(6)	108.1(4)
C2B–N3B–C4B	109.4(4)	107.8(5)	109.3(3)	108.7(7)	108.8(4)
N3A–C4A–C5A	102.5(2)	102.1(5)	100.9(3)	104.6(6)	101.0(4)
N3B–C4B–C5B	102.7(4)	102.4(4)	102.6(3)	104.7(7)	102.9(4)
C4A–C5A–N1A	104.1(2)	104.3(5)	103.9(3)	104.3(6)	103.6(4)
C4B–C5B–N1B	105.1(4)	104.7(5)	104.5(3)	105.3(7)	104.7(4)
C5A–N1A–C2A	109.8(2)	109.5(5)	110.0(3)	111.4(6)	110.3(4)
C5B–N1B–C2B	110.9(4)	109.9(5)	111.1(3)	110.7(7)	111.5(4)
N1A–C2A–O6A	126.9(2)	125.9(5)	128.2(3)	129.2(7)	127.1(5)
N1B–C2B–O6B	126.7(5)	127.8(5)	126.7(3)	128.3(7)	126.4(5)
N3A–C2A–O6A	121.2(2)	122.2(5)	121.4(3)	120.5(6)	121.3(5)
N3B–C2B–O6B	121.5(5)	120.4(5)	122.5(3)	128.3(7)	121.8(4)
C2A–N3A–C9A–C11A	–19.9(9)	8.2(9)	24.1(5)	–1.5(12)	23.0(8)
C2B–N3B–C9B–C11B	–15.9(8)	13.9(9)	9.8(5)	2.2(16)	6.0(8)
N1A–C5A–C7A–O8A	–47.0(7)	–10.5(9)	147.1(5)	95.7(9)	–22.5(7)
N1B–C5B–C7B–O8B	–54.6(7)	176(3)	93.8(4)	–34.1(12)	136.8(5)

^a Refer to Table 1 for atom labels. Data for Rh₂(4S-MPPIM)₄ (**1**) are provided for comparison.¹¹ The values in parentheses are the estimated standard deviations and were calculated by $\sigma_{\text{av}} = [1/(\sum_i(1/\sigma_i))]^{1/2}$, where σ_i is the estimated standard deviation of each angle contributing to the average.

When viewed along the rhodium–rhodium bond, the BSPIM catalysts (Figure 4) also correspond to the depiction offered in Figure 1. Although the twist of the phenylsulfonyl groups on the ligands makes the determination less clear, Rh₂(4S,2'S-BSPIM)₄ (**15**) corresponds to the “matched” case, with the ligands’ tetrahydropyrrole rings and pendant methyl esters are oriented in the same helical sense (*M*).²² In the diastereomeric Rh₂(4S,2'R-BSPIM)₄ (**16**) the configuration of the pendant methyl esters and *N*-prolinate attachment are opposed to each other, making this catalyst the “mismatched” example.

Match/Mismatch Selectivity. Because dirhodium(II) carboxamidates catalyze highly enantioselective and diastereoselective intramolecular C–H insertion reactions with diazoacetates, three model reactions were surveyed: (1) diazo decomposition of cyclohexyl diazoacetate (Table 3), which exhibits both diastereoselectivity and enantioselectivity;²³ (2) a similar reaction with cyclopentyl diazoacetate (Table 4), where enantioselectivity in C–H insertion beyond 93% ee has not been achieved with any chiral catalyst;²⁴ and (3) cyclization with the acyclic 2-methoxy-1-ethyl diazoacetate (Table

5),²⁵ which has more degrees of freedom in its orientation for reactions. A distinct “match/mismatch” phenomenon is evident in the enantioselectivities obtained from these reactions: the “matched” cases result in equal or greater enantiomeric excesses in comparison to the ee's obtained with the known Rh₂(4S-MPPIM)₄. Conversely, the “mismatched” cases result in significantly lower enantiomeric excesses. Particularly large match/mismatch effects are noted in the cases of the BSPIM catalysts with a maximum difference of 88% ee for the C–H insertion reactions of 2-methoxy-1-ethyl diazoacetate. Presumably, the closer proximity of the large *N*-acyl side chain in Rh₂(BSPIM)₄ to the axial active site gives these catalysts greater enantiodiscriminating capabilities. However, diastereoselectivity (*cis/trans* ratio, Table 3) is not subject to the same influences as is enantioselectivity, and **12** appears to be the only catalyst from which a significant impact is realized.

In contrast, model intra- and intermolecular cyclopropanation reactions did not show the same selectivity trends as those observed for the C–H insertions (Tables 6 and 7). Intramolecular cyclopropanation of methallyl

(22) For a discussion of helical chirality, see: Eliel, E. L.; Wilen, S. H. *Stereochemistry of Organic Compounds*; Wiley: New York, 1994.

(23) Doyle, M. P.; Dyatkin, A. B.; Roos, G. H. P.; Canas, F.; Pierson, D. A. *J. Am. Chem. Soc.* **1994**, *116*, 4507–4508.

(24) Doyle, M. P.; Zhou, Q.-L.; Dyatkin, A. B.; Ruppert, D. A. *Tetrahedron Lett.* **1995**, *36*, 7579–7582.

(25) Doyle, M. P.; van Oeveren, A.; Westrum, L. J.; Protopopova, M. N.; Clayton, T. W., Jr. *J. Am. Chem. Soc.* **1991**, *113*, 8982–8984.

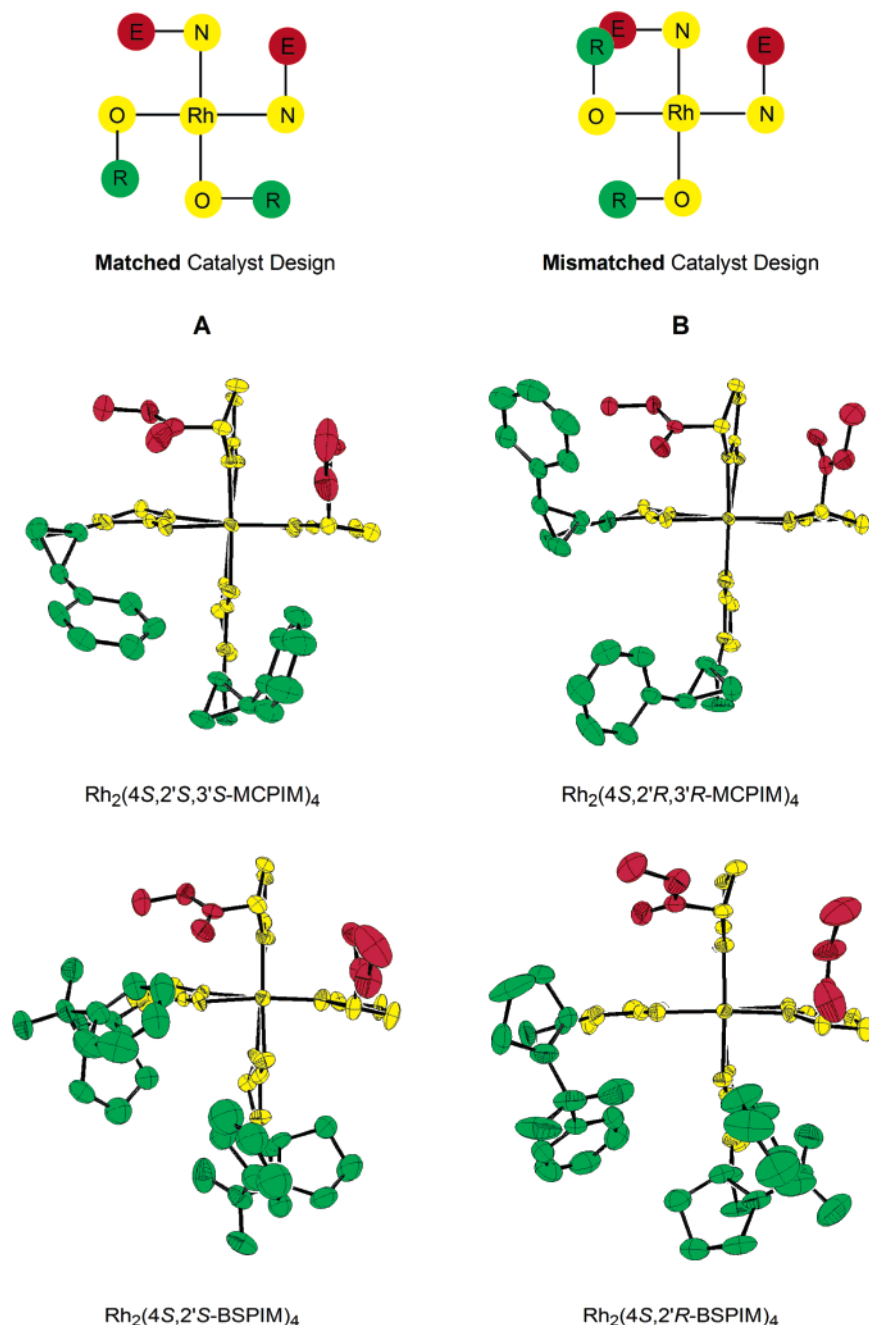


FIGURE 4. Configurational differences with chiral *N*-acyl groups in imidazolidinone-ligated dirhodium(II) carboxamidate catalysts. Each catalyst structure is viewed down the length of the rhodium–rhodium bond. Only the pendant groups around the front rhodium atom are shown; axial ligands are removed for clarity. Thermal ellipsoids are scaled to 50% probability.

diazoacetate was chosen because use of $\text{Rh}_2(4S\text{-MPPIM})_4$ gave the highest % ee value for this process of any chiral catalyst yet examined.²⁴ Although the catalysts described here give rise to lower enantioselectivities than does **1**, the match/mismatch phenomenon continues to hold. The intermolecular cyclopropanation reaction of styrene with ethyl diazoacetate offers an overview of diastereoselectivity as well as enantioselectivity, but this reaction has generally resisted high levels of stereocontrol.²⁶ In both

cases the % ee of the predominant *cis* product was lower in comparison to the selectivity arising from $\text{Rh}_2(4S\text{-MPPIM})_4$, and diastereoselectivity was also low.

Lower enantioselectivities relative to $\text{Rh}_2(4S\text{-MPPIM})_4$ are also observed for hetero-Diels–Alder (HDA) reactions of the Danishefsky diene with either *p*-nitrobenzaldehyde (Table 8) or 5-nitro-2-thiophenecarboxaldehyde (Table 9).¹⁷ These aldehydes were selected because of their high reactivity with the $\text{Rh}_2(4S\text{-MPPIM})_4$ catalyst. The high product yields suggest that all cycloaddition product is formed via the catalytic pathway.²⁷ However, in neither

(26) For exceptions using the chiral azetidinone-ligated dirhodium(II) catalysts, see: (a) Doyle, M. P.; Davies, S. B.; Hu, W. *Chem. Commun.* **2000**, 867–868. (b) Doyle, M. P.; Zhou, Q.-L.; Simonsen, S. H.; Lynch, V. *Synlett* **1996**, 697–698.

(27) Estimated rates for these processes were 100-fold greater than those for the background uncatalyzed reactions.

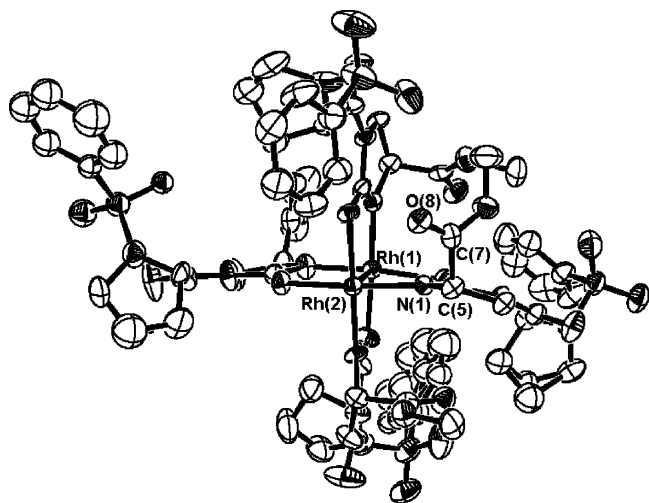
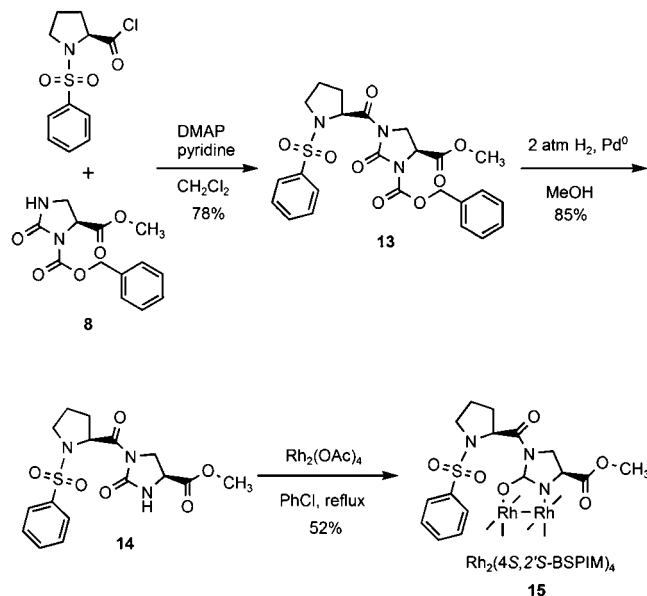


FIGURE 5. ORTEP plot of $(cis-2,2)-[Rh_2(4S,2'S-BSPIM)_4(CH_3OH)_2]$ (**15**) showing a partial atom labeling scheme. The axial ligands have been removed for clarity. Thermal ellipsoids are scaled to the 50% probability level.

SCHEME 3. Synthesis of $(cis-2,2)-Rh_2(4S,2'S-BSPIM)_4$ (15**). Complex **16**, $(cis-2,2)-Rh_2(4S,2'R-BSPIM)_4$, Is Produced Analogously from *R*-Proline**



case does enantioselectivity for product formation approach that achieved with the use of $Rh_2(4S-MPPIM)_4$. Curiously, with the “matched” catalysts **11** and **15** there is lower enantiocontrol than with the “mismatched” catalysts **12** and **16**. This selectivity change underscores the fact that configurational changes in the catalyst affect the HDA and metal carbene reactions in unique ways, depending on their respective reaction mechanisms.

Implications for Stereoselectivity. The mechanisms of both metal carbene C–H insertion²⁸ and cyclopropanation²⁹ reactions are reasonably well under-

(28) Nakamura, E.; Yoshikai, N.; Yamanaka, M. *J. Am. Chem. Soc.* **2002**, *124*, 7181–7192. (b) Davies, H. M. L.; Beckwith, R. E. *J. Chem. Rev.* **2003**, *103*, 2861–2904. (c) Pirrung, M. C.; Liu, H.; Morehead, A. T., Jr. *J. Am. Chem. Soc.* **2002**, *124*, 1014–1023.

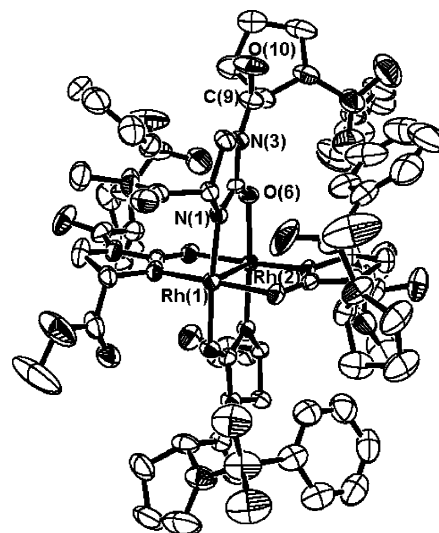


FIGURE 6. ORTEP plot of $(cis-2,2)-[Rh_2(4S,2'R-BSPIM)_4-(CH_3CN)(PhCN)]$ (**16**) showing a partial atom labeling scheme. The axial ligands have been removed for clarity. Thermal ellipsoids are scaled to the 50% probability level.

TABLE 3. Carbon–Hydrogen Insertion Reaction of Cyclohexyl Diazoacetate^a

catalyst	yield (%) ^b	<i>cis/trans</i> ^c	% ee <i>cis</i> ^c	% ee <i>trans</i> ^c
$Rh_2(4S-MPPIM)_4$, 1	71	100/0	92	na
$Rh_2(4S,2'S,3'S-MCPIM)_4$, 11	78	99/1	97	nd
$Rh_2(4S,2'R,3'R-MCPIM)_4$, 12	63	80/20	72	13
$Rh_2(4S,2'S-BSPIM)_4$, 15	88	97/3	>99	>99
$Rh_2(4S,2'R-BSPIM)_4$, 16	89	98/2	74	33

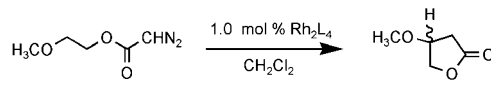
^a Reactions performed in refluxing CH_2Cl_2 using 1.0 mol % catalyst. ^b Reported as isolated yields after column chromatography. ^c *cis/trans* ratios and enantiomeric excesses were determined by gas chromatography.

TABLE 4. Carbon–Hydrogen Insertion Reaction of Cyclopentyl Diazoacetate^a

catalyst	yield (%) ^b	% ee ^c
$Rh_2(4S-MPPIM)_4$, 1	67	93 ^d
$Rh_2(4S,2'S,3'S-MCPIM)_4$, 11	81	88
$Rh_2(4S,2'R,3'R-MCPIM)_4$, 12	75	40
$Rh_2(4S,2'S-BSPIM)_4$, 15	78	98
$Rh_2(4S,2'R-BSPIM)_4$, 16	62	22

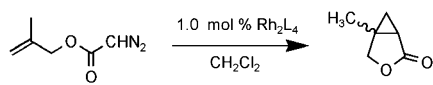
^a Reactions performed in refluxing CH_2Cl_2 using 1.0 mol % catalyst. ^b Reported as isolated yields after column chromatography. ^c Enantiomeric excesses were determined by gas chromatography. ^d Reference 24.

stood.^{12,13,18} More recently the mechanism of the hetero-Diels–Alder reaction catalyzed by dirhodium(II) carboxamidates has been unraveled.^{17b,c} Accordingly, in reactions catalyzed by dirhodium(II) compounds, the four bridging ligands are assumed to remain bound to the dirhodium

TABLE 5. Carbon–Hydrogen Insertion Reaction of 2-Methoxyethyl Diazoacetate^a


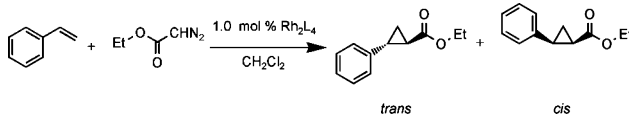
catalyst	yield (%) ^b	% ee ^c
Rh ₂ (4 <i>S</i> -MPPIM) ₄ , 1	50	92
Rh ₂ (4 <i>S</i> ,2' <i>S</i> ,3' <i>S</i> -MCPIM) ₄ , 11	69	91
Rh ₂ (4 <i>S</i> ,2' <i>R</i> ,3' <i>R</i> -MCPIM) ₄ , 12	64	46
Rh ₂ (4 <i>S</i> ,2' <i>S</i> -BSPIM) ₄ , 15	72	94
Rh ₂ (4 <i>S</i> ,2' <i>R</i> -BSPIM) ₄ , 16	72	6

^a Reactions performed in refluxing CH₂Cl₂ using 1.0 mol % catalyst. ^b Reported as isolated yields after column chromatography. ^c Enantiomeric excesses were determined by gas chromatography.

TABLE 6. Intramolecular Cyclopropanation with 3-Methylbutenyl Diazoacetate^a


catalyst	yield (%) ^b	% ee ^c
Rh ₂ (4 <i>S</i> -MPPIM) ₄ , 1	75	89 ^d
Rh ₂ (4 <i>S</i> ,2' <i>S</i> ,3' <i>S</i> -MCPIM) ₄ , 11	70	80
Rh ₂ (4 <i>S</i> ,2' <i>R</i> ,3' <i>R</i> -MCPIM) ₄ , 12	65	52
Rh ₂ (4 <i>S</i> ,2' <i>S</i> -BSPIM) ₄ , 15	58	80
Rh ₂ (4 <i>S</i> ,2' <i>R</i> -BSPIM) ₄ , 16	70	16

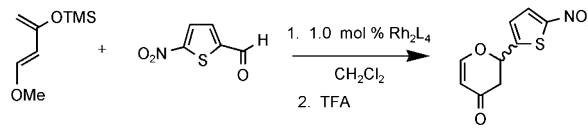
^a Reactions performed in refluxing CH₂Cl₂ using 1.0 mol % catalyst. ^b Reported as isolated yields after column chromatography. ^c Enantiomeric excesses were determined by gas chromatography. ^d Reference 24.

TABLE 7. Intermolecular Cyclopropanation of Styrene with Ethyl Diazoacetate^a


catalyst	yield (%) ^b	<i>cis/trans</i> ^c	% ee	
			<i>cis</i> ^c	<i>trans</i> ^c
Rh ₂ (4 <i>S</i> -MPPIM) ₄ , 1	64	74/26	45	3
Rh ₂ (4 <i>S</i> ,2' <i>S</i> ,3' <i>S</i> -MCPIM) ₄ , 11	70	62/38	18	14
Rh ₂ (4 <i>S</i> ,2' <i>R</i> ,3' <i>R</i> -MCPIM) ₄ , 12	59	49/51	21	68
Rh ₂ (4 <i>S</i> ,2' <i>S</i> -BSPIM) ₄ , 15	58	58/42	38	24
Rh ₂ (4 <i>S</i> ,2' <i>R</i> -BSPIM) ₄ , 16	48	63/37	31	29

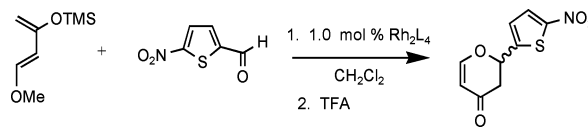
^a Reactions performed in refluxing CH₂Cl₂ using 1.0 mol % catalyst. ^b Reported as isolated yields after column chromatography. ^c *cis/trans* ratios and enantiomeric excesses were determined by gas chromatography.

core, and the catalyzed transformation takes place at the axial coordination site without disturbing ligand binding on rhodium. This presumption has been borne out by diverse examples of catalyst stability through uniform selectivity in multiple use-reuse for applications with diazoacetates.^{30,31} Carboxamidate ligands undergo slow exchange at 70 °C,³¹ so at the temperatures used to evaluate the catalyst series in this study (40 °C and

TABLE 8. Hetero-Diels–Alder Reaction between Danishefsky's Diene and *p*-Nitrobenzaldehyde^a


catalyst	yield (%) ^b	% ee ^c
Rh ₂ (4 <i>S</i> -MPPIM) ₄ , 1	82	95 ^d
Rh ₂ (4 <i>S</i> ,2' <i>S</i> ,3' <i>S</i> -MCPIM) ₄ , 11	83	48
Rh ₂ (4 <i>S</i> ,2' <i>R</i> ,3' <i>R</i> -MCPIM) ₄ , 12	93	82
Rh ₂ (4 <i>S</i> ,2' <i>S</i> -BSPIM) ₄ , 15	80	73
Rh ₂ (4 <i>S</i> ,2' <i>R</i> -BSPIM) ₄ , 16	93	59

^a Reactions performed at room temperature in CH₂Cl₂ with 1.0 mol % catalyst. The reaction was quenched after 48 h by adding neat trifluoroacetic acid. ^b Reported as isolated yields after column chromatography. ^c Enantiomeric excesses were determined by HPLC (Chiracel OD column). ^d Reference 17a.

TABLE 9. Hetero-Diels–Alder Reaction between Danishefsky's Diene and 5-Nitro-2-thiophenecarboxaldehyde^a


catalyst	yield (%) ^b	% ee ^c
Rh ₂ (4 <i>S</i> -MPPIM) ₄ , 1	81	94 ^d
Rh ₂ (4 <i>S</i> ,2' <i>S</i> ,3' <i>S</i> -MCPIM) ₄ , 11	80	55
Rh ₂ (4 <i>S</i> ,2' <i>R</i> ,3' <i>R</i> -MCPIM) ₄ , 12	85	75
Rh ₂ (4 <i>S</i> ,2' <i>S</i> -BSPIM) ₄ , 15	86	77
Rh ₂ (4 <i>S</i> ,2' <i>R</i> -BSPIM) ₄ , 16	95	55

^a Reactions performed at room temperature in CH₂Cl₂ with 1.0 mol % catalyst. The reaction was quenched after 48 h by adding neat trifluoroacetic acid. ^b Reported as isolated yields after column chromatography. ^c Enantiomeric excesses were determined by HPLC (Chiracel OD column). ^d Reference 17a.

lower) the rate for carboxamidate ligand exchange is negligible. Furthermore, when a ligand is removed from the dirhodium core, as occurs in catalytic reactions with organosilanes,³² the dirhodium(II) framework does not remain intact, and the reactant catalyst cannot be recovered.

Results from the matched/mismatched cases presented in Tables 3–7 show consistent behavior across a variety of C–H insertion and cyclopropanation substrates, consistent with the intact dirhodium(II) tetracarboxamidates. For these diazo decomposition reactions, the matched cases exhibit higher enantiocontrol for all reactions under consideration, and use of the mismatched catalysts leads to lower stereoselectivity. Such consistency across substrates with different steric and electronic requirements is unlikely if ligand dissociation and/or rearrangement were to occur. With the Lewis acid catalyzed reactions in Tables 8 and 9, where there is no

(29) (a) Nowlan, D. T., III; Gregg, T. M.; Davies, H. M. L.; Singleton, D. A. *J. Am. Chem. Soc.* **2003**, *125*, 15902–15911. (b) Fraile, J. M.; Garcia, J. I.; Martinez-Merino, V.; Mayoral, J. A.; Salvatella, L. *J. Am. Chem. Soc.* **2001**, *123*, 7616–7625. (c) Müller, P.; Bernardinelli, G.; Allenbach, Y. F.; Ferri, M.; Flack, H. D. *Org. Lett.* **2004**, *6*, 1725–1728. (d) Davies, H. M. L.; Antoulinakis, E. G. *Org. React.* **2001**, *57*, 1–326.

(30) (a) Doyle, M. P.; Yan, M.; Gau, H.-M.; Blosssey, E. C. *Org. Lett.* **2003**, *5*, 561–563. (b) Doyle, M. P.; Timmons, D. J.; Tumonis, J. S.; Gau, H.-M.; Blosssey, E. C. *Organometallics* **2002**, *21*, 1747–1749. (c) Nagashima, T.; Davies, H. M. L. *Org. Lett.* **2002**, *4*, 1989–1992. (d) Davies, H. M. L.; Walji, A. M.; Nagashima, T. *J. Am. Chem. Soc.* **2004**, *126*, 4271–4280.

(31) Doyle, M. P.; Eismont, M. Y.; Bergbreiter, D. E.; Gray, H. N. *J. Org. Chem.* **1992**, *57*, 6103–6105.

(32) Doyle, M. P.; Shanklin, M. S. *Organometallics* **1994**, *13*, 1081–1088.

evidence of ligand disruption from extensive studies in which carboxamidate catalysts are closely monitored,^{17b,c} uniform and reproducible results are obtained that are fully consistent with intact dirhodium(II) exhibiting four bridging carboxamidate ligands.

Conclusion. The structural rigidity of the two pairs of diastereomeric rhodium(II) carboxamidate catalysts aids in understanding their role in asymmetric catalysis. Intramolecular reactions are more profoundly affected than are intermolecular reactions, consistent with the operational sense of a tethered substrate in a rotor. When orientation of the two chiral attachments is complimentary, stereochemical enhancement occurs; when opposed, stereochemically destructive interference occurs. Intermolecular reactions have more degrees of freedom in their orientations, and the outcome is a lower overall effect on stereocontrol. This has been a characteristic of the (*cis*-2,2)-dirhodium(II) carboxamidate catalysts; they are more versatile (higher stereocontrol) toward intramolecular reactions than intermolecular reactions.^{12,13} A surprising outcome of this study is the demonstration that Rh₂(4*S*-MPPIM)₄ operates very close to optimum selectivity for overall stereocontrol. The placement of the two carboxylate substituents around the axial coordination site is sufficient to reach high levels of enantiocontrol, and only incremental enhancements are achieved by further manipulations.

Experimental Section

Methyl 1-[3'(S)-Phenyl-2'(S)-cyclopropanecarbonyl]-2-oxo-imidazolidine-4(S)-carboxylate, (4*S*,2'*S*,3'*S*)-HMCPIM (S,S,S-10). A 250 mL round-bottom flask was charged with methyl 3-benzyloxycarbonyl-2-oxo-imidazolidine-4(S)-carboxylate **8** (4.50 g, 16.2 mmol), 4-(dimethylamino)pyridine (DMAP, 0.190 g, 1.60 mmol), pyridine (3.3 mL, 32.4 mmol), and 75 mL of distilled dichloromethane. The reaction vessel was then flushed with nitrogen and cooled to 0 °C. A solution of **7** (3.50 g, 19.4 mmol) in 20 mL of dichloromethane was added dropwise over 30 min via syringe pump and the reaction was allowed to stir at 0 °C for an additional 30 min. The solution was heated to reflux, turning brown over 16 h. An additional 200 mL of dichloromethane was added to the solution, which was subsequently washed with aqueous solutions of cold 1 M HCl (2 × 50 mL), saturated NaHCO₃ (1 × 50 mL), and saturated brine (1 × 50 mL). The solution was then dried with anhydrous MgSO₄, filtered, and concentrated under reduced pressure to afford an orange foam, which was subsequently purified via column chromatography (SiO₂; ethyl acetate/hexanes 1:1) to yield 5.88 g of a 1:1 mixture of **S,S,S-9** and **S,R,R-9** as a white solid (13.9 mmol, 86% yield) which was used immediately in the next step. Characterization data for compound **S,R,R-9**: ¹H NMR (300 MHz, CDCl₃) δ 7.38–7.13 (comp, 10 H), 5.38 (d, *J* = 12.2 Hz, 1 H), 5.24 (d, *J* = 12.2 Hz, 1 H), 4.71 (dd, *J* = 10.0, 3.7 Hz, 1 H), 4.00 (dd, *J* = 12.2, 10.0 Hz, 1 H), 3.90 (dd, *J* = 12.2, 3.7 Hz, 1 H), 3.70 (s, 3 H), 3.59 (ddd, *J* = 8.3, 5.1, 4.4 Hz, 1 H), 2.68 (ddd, *J* = 9.3, 6.6, 4.4 Hz, 1 H), 1.71 (ddd, *J* = 9.3, 5.1, 4.2 Hz, 1 H), 1.46 (ddd, *J* = 8.3, 6.6, 4.2 Hz, 1 H); ¹³C NMR (75 MHz, CDCl₃) δ 173.0, 169.4, 150.8, 149.5, 139.6, 134.6, 128.6, 128.4, 128.3, 126.6, 126.3, 68.9, 53.1, 52.1, 42.7, 28.8, 23.6, 19.5. Mp 101–102 °C. [α]²⁴_D = –143.6 (c 0.1, CH₂Cl₂). HRMS for (C₂₃H₂₃N₂O₆)⁺ theoretical 423.1551 [M + H]⁺; found 423.1562.

A round-bottom flask was charged with a 1:1 mixture of **S,S,S-9** and **S,R,R-9** (5.00 g, 11.8 mmol) and 50 mL of dry ethyl acetate and placed under argon. Palladium black (10 mg, 0.094 mmol) was added, and the solution was placed under hydrogen (balloon pressure) and stirred for 90 min. The resulting mixture was filtered through Celite with dichlo-

romethane wash and concentrated under reduced pressure to produce an off-white solid that was purified by column chromatography (ethyl acetate/hexanes 1:1) that separated the two diastereoisomers of **10** and afforded 1.33 g of **S,S,S-10** as a white solid (4.60 mmol, 67% yield over two steps), *R*_f = 0.40. Compound **S,S,S-10** was recrystallized by slow evaporation of a dichloromethane/hexanes solution prior to use in further reactions. ¹H NMR (400 MHz, CDCl₃) δ 7.30–7.24 (comp, 2 H), 7.21–7.13 (comp, 3 H), 5.65 (br s, 1 H), 4.28–4.24 (m, 1 H), 4.15 (d, *J* = 7.6 Hz, 2 H), 3.79 (s, 3 H), 3.62 (ddd, *J* = 8.3, 5.3, 4.4 Hz, 1 H), 2.65 (ddd, *J* = 9.3, 6.6, 4.4 Hz, 1 H), 1.70 (ddd, *J* = 9.3, 5.3, 4.4 Hz, 1 H), 1.38 (ddd, *J* = 8.3, 6.6, 4.4 Hz, 1 H); ¹³C NMR (100 MHz, CDCl₃) δ 172.8, 170.7, 155.6, 140.1, 128.4, 126.4, 126.2, 53.1, 49.4, 45.4, 28.2, 22.9, 18.7. Mp 167–168 °C. [α]²⁴_D = +223.5 (c 0.1, CH₂Cl₂). HRMS for (C₁₅H₁₇N₂O₄)⁺ theoretical 289.1188 [M + H]⁺; found 289.1179. Anal. Calcd for C₁₅H₁₆N₂O₄: 62.49 C, 5.59 H, 9.72 N. Found: 62.57 C, 5.80 H, 9.32 N.

Methyl 1-[3'(R)-Phenyl-2'(R)-cyclopropanecarbonyl]-2-oxo-imidazolidine-4(S)-carboxylate, (4*S*,2'*R*,3'*R*)-HMCPIM (S,R,R-10) was separated from the diastereomeric mixture of **10**, as described above, and purified by column chromatography (hexanes/ethyl acetate 1:1, *R*_f = 0.31) to produce 1.19 g of a white solid (4.13 mmol, 60% yield over two steps): ¹H NMR (300 MHz, CDCl₃) δ 7.29–7.14 (comp, 5 H), 5.87 (br s, 1 H), 4.25 (t, *J* = 7.3 Hz, 1 H), 4.14 (d, *J* = 7.3 Hz, 2 H), 3.77 (s, 3 H), 3.62 (ddd, *J* = 8.4, 5.1, 4.4 Hz, 1 H), 2.64 (ddd, *J* = 9.3, 6.6, 4.4 Hz, 1 H), 1.70 (ddd, *J* = 9.3, 5.1, 4.2 Hz, 1 H), 1.38 (ddd, *J* = 8.4, 6.6, 4.2 Hz, 1 H); ¹³C NMR (75 MHz, CDCl₃) δ 172.8, 170.7, 155.6, 140.1, 128.4, 126.5, 53.0, 49.4, 45.4, 28.1, 23.0, 18.8. Mp 91–92 °C. [α]²⁴_D = –211.6 (c 0.1, CH₂Cl₂). HRMS for (C₁₅H₁₇N₂O₄)⁺ theoretical 289.1188 [M + H]⁺; found 289.1194.

Dirhodium(II) Tetrakis{methyl 1-[3'(S)-phenyl-2'(S)-cyclopropanecarbonyl]-2-oxo-imidazolidine-4(S)-carboxylate}, (*cis*-2,2)-[Rh₂(4*S*,2'*S*,3'*S*-MCPIM)₄(CH₃CN)(CH₃OH)] (11). A 25 mL two-neck round-bottom flask, stirbar, Soxhlet extractor, and condenser were flame-dried and assembled under a constant flow of argon while still warm, sealing all ground glass joints with Teflon tape. A cellulose extraction thimble filled with an oven-dried mixture of sodium carbonate and sand (2:1) was capped with glass wool and placed in the Soxhlet extractor during assembly. Dirhodium(II) acetate (200 mg, 0.452 mmol), **S,S,S-10** (1.04 g, 3.62 mmol), and 15.0 mL of anhydrous chlorobenzene were added though the open neck of the flask, which was sealed with a septum and then heated at reflux for 17 h with a 1 min solvent flush rate through the Soxhlet extractor. The progress of the ligand exchange reaction was monitored by HPLC using a 3.9 mm × 150 mm reverse-phase μ-Bondapak-CN column. When conversion to product was complete (by HPLC), the reaction mixture was cooled to room temperature and concentrated to a purple oil. The crude material was purified by column chromatography on reverse phase Bakerbond CN resin (100% methanol to 99:1 methanol/ acetonitrile), and the first red band was collected. Solvent was removed under reduced pressure to produce a red solid. This (2,2-*cis*) isomer (**11**) was recrystallized by slow evaporation from a warm methanol solution containing a small amount of acetonitrile to afford 374 mg of red crystals (0.276 mmol, 61% yield). ¹H NMR (400 MHz, CD₃CN) δ 7.44–7.40 (comp, 4 H), 7.35–7.30 (comp, 2 H), 7.27–7.23 (comp, 8 H), 7.14–7.07 (comp, 6 H), 3.94 (dd, *J* = 8.7, 2.8 Hz, 2 H), 3.88–3.77 (comp, 4 H), 3.75 (s, 6 H), 3.73–3.64 (comp, 4 H), 3.60 (s, 6 H), 3.57–3.53 (comp, 2 H), 3.46 (dd, *J* = 11.5, 4.8 Hz, 2 H), 3.35 (ddd, *J* = 8.5, 5.2, 4.4 Hz, 2 H), 2.37 (ddd, *J* = 9.5, 6.4, 4.4 Hz, 2 H), 2.31 (ddd, *J* = 9.5, 6.4, 4.4 Hz, 2 H), 1.96 (s, 6 H), 1.61 (ddd, *J* = 9.1, 5.2, 3.6 Hz, 2 H), 1.40 (ddd, *J* = 9.1, 5.2, 4.0 Hz, 2 H), 1.08 (ddd, *J* = 8.3, 6.4, 3.6 Hz, 2 H), 0.96 (ddd, *J* = 8.3, 6.4, 4.0 Hz, 2 H); ¹³C NMR (100 MHz, CD₃CN) δ 175.0, 173.7, 171.1, 170.8, 166.5, 166.1, 142.2, 142.1, 129.4, 129.3, 128.3, 127.6, 127.4, 118.4, 60.5, 59.9, 53.1, 52.5, 48.5, 48.0, 28.8, 28.4, 23.1, 22.2, 18.2, 16.9. [α]²⁴_D = –248.4 (c 0.1, CH₂Cl₂). HRMS

for (CsRh₂C₆₀H₆₀N₈O₁₆⁺) theoretical 1487.1292 [M + Cs]⁺; found 1487.1329. Anal. Calcd for Rh₂C₆₅H₇₀N₁₀O₁₇: 53.14 C, 4.80 H, 9.53 N (includes 1 acetonitrile molecule per catalyst molecule in addition to axial MeCN and MeOH ligands). Found: 53.12 C, 4.84 H, 9.56 N.

X-ray Structure of 11. Crystals grew as red plates from dry methanol/acetonitrile (99:1). The data crystal had approximately orthogonal dimensions 0.41 × 0.21 × 0.03 mm³. Crystals of **11** (Rh₂C₆₆H₇₈N₉O₂₁, containing one methanol and one acetonitrile molecule coordinated in the axial sites) were orthorhombic, space group *P*2(1)2(1)2(1), with *a* = 10.6025(4), *b* = 17.5485(6), *c* = 37.3067(13) Å, *V* = 6941.2(4) Å³, *Z* = 4, ρ(calc) = 1.473 Mg m⁻³. The unit cell additionally contained 3 molecules of methanol and 1 molecule of water. Data were collected out to 2θ = 55.03° by the ω-scan technique at -100 °C using graphite-monochromatized Mo Kα radiation (λ = 0.71073 Å); 78592 reflections were measured of which 15585 were unique [R_{int}(*F*²) = 0.0714]. The structure was solved by direct methods and refined by full-matrix least-squares on *F*² with anisotropic displacement parameters for the non-hydrogen atoms. The hydrogen atoms were calculated and placed in idealized positions throughout the refinement and convergence process. The final R_w(*F*²) = 0.1327 with a goodness of fit = 1.055 for refining 839 parameters. The conventional R(*F*) = 0.1029 for 11057 reflections for *F*_o > 2σ(*F*_o). Data reduction, decay correction, structure solution, and refinement were done using the SHELXTL/PC software package.³³ An absorption correction was applied with the SADABS program.³⁴ Tables of positional and thermal parameters, bond lengths and angles, and torsion angles and figures are located in a CIF file as Supporting Information.

Dirhodium(II) Tetrakis{methyl 1-[3'(R)-phenyl-2'(R)-cyclopropanecarbonyl]-2-oxo-imidazolidine-4(S)-carboxylate}, (cis-2,2)-[Rh₂(4S,2'R,3'R-MCPIM)₄(CH₃OH)₂] (12) was prepared analogously to the procedure reported for compound **11**. The (2,2-*cis*) isomer **12** was recrystallized from undried methanol with trace acetonitrile (405 mg, 0.30 mmol, 53% yield). ¹H NMR (400 MHz, CD₃CN) δ 7.37–7.19 (comp, 14 H), 7.17–7.10 (comp, 2 H), 7.06–7.01 (comp, 4 H), 4.22 (dd, *J* = 10.7, 5.2 Hz, 2 H), 3.99 (dd, *J* = 11.1, 10.7 Hz, 2 H), 3.83 (dd, *J* = 9.5, 2.2 Hz, 2 H), 3.80–3.63 (comp, 2 H), 3.76 (br s, 12 H), 3.60 (dd, *J* = 10.7, 2.2 Hz, 2 H), 2.98 (s, 6 H), 2.46 (ddd, *J* = 9.5, 6.4, 4.4 Hz, 2 H), 2.37 (ddd, *J* = 9.5, 6.4, 4.4 Hz, 2 H), 2.15 (s, 6 H), 1.62 (ddd, *J* = 9.1, 5.2, 4.0 Hz, 2 H), 1.24 (ddd, *J* = 8.6, 6.4, 4.0 Hz, 2 H), 1.13 (ddd, *J* = 9.1, 5.2, 4.0 Hz, 2 H), 0.69 (ddd, *J* = 8.6, 6.4, 4.0 Hz, 2 H); ¹³C NMR (100 MHz, CD₃CN) δ 175.1, 173.3, 170.8, 166.0, 142.4, 141.8, 129.4, 129.3, 127.5, 127.4, 127.3, 127.2, 60.5, 60.2, 53.3, 51.9, 50.0, 48.5, 48.2, 28.2, 27.0, 24.0, 23.9, 23.7, 19.4, 18.3. [α]_D²⁴ = -331.8 (*c* 0.1, CH₃CN). HRMS for (Rh₂C₆₀H₆₀N₈O₁₆)⁺, theoretical 1354.2237 [M]⁺; found 1354.2337. Anal. Calcd for Rh₂C₆₀H₆₄N₈O₁₈ (containing 2 molecules of water as axial ligands): 51.81 C, 4.64 H, 8.06 N. Found: 51.85 C, 5.04 H, 8.27 N.

X-ray Structure of 12. Crystals grew as red prisms from dry methanol/acetonitrile (98:2). The data crystal had approximately orthogonal dimensions 0.42 × 0.31 × 0.23 mm³. Crystals of **12** (Rh₂C₆₂H₆₈N₈O₁₈, containing 2 molecules of methanol coordinated in the axial sites) were orthorhombic, space group *P*2(1)2(1)2(1), with *a* = 10.8222(14), *b* = 21.851(3), *c* = 30.510(4) Å, *V* = 7214.9(16) Å³, *Z* = 4, ρ(calc) = 1.424 Mg m⁻³. Data were collected out to 2θ = 56.10° by the ω-scan technique at -100 °C using graphite-monochromatized Mo Kα radiation (λ = 0.71073 Å); 90,349 reflections were measured of which 16,592 were unique [R_{int}(*F*²) = 0.0523]. The structure was solved by direct methods and refined by full-matrix least-squares on *F*² with anisotropic displacement parameters for the non-hydrogen atoms. The hydrogen atoms were calculated and placed in idealized positions throughout the refinement

and convergence process. The final R_w(*F*²) = 0.0856 with a goodness of fit = 1.001 for refining 897 parameters. The conventional R(*F*) = 0.0367 for 15,086 reflections for *F*_o > 2σ(*F*_o). Data reduction, decay correction, structure solution, and refinement were done using the SHELXTL/PC software package.³⁵ An absorption correction was applied with the SADABS program.³⁴ Tables of positional and thermal parameters, bond lengths and angles, and torsion angles and figures are located in a CIF file as Supporting Information.

Methyl 1-[1-Benzenesulfonyl-pyrrolidine-2'(S)-carboxyl]-3-benzoyloxycarbonyl-2-oxo-imidazolidine-4(S)-carboxylate (S,S-13). A round-bottom flask was charged with (S)-*N*-benzenesulfonylproline (1.0 g, 3.95 mmol) and anhydrous THF (25 mL) and cooled to -78 °C. To this solution was added triethylamine (0.44 g, 4.34 mmol, 1.1 equiv) and pivaloyl chloride (0.52 g, 4.34 mmol, 1.1 equiv). The resulting milky white mixture was allowed to stir at -78 °C for 30 min and then at 0 °C for 90 min. The temperature was then lowered to -78 °C, while the lithiated imidazolidine solution is prepared as follows: in a separate flask, a solution of **8** (0.724 g, 2.60 mmol) in THF (25 mL) was treated with *n*-butyllithium (1.0 equiv, 2.5 M in hexanes) at -78 °C and allowed to stir for 30 min. The resulting solution of the lithium salt was added via cannula to the proline acid chloride solution at -78 °C. After stirring overnight at room temperature, the reaction mixture was washed with saturated Na₂CO₃ and extracted five times with ethyl acetate. The organic layers were combined, and the solvent removed under reduced pressure. The resulting pale yellow solid was purified on a silica plug yielding a white solid that was used immediately in the next step (1.04 g, 2.02 mmol, 78% yield). ¹H NMR (300 MHz, CDCl₃) δ 7.82–7.87 (comp, 2 H), 7.55–7.42 (comp, 3 H), 7.35–7.26 (comp, 5 H), 5.68 (dd, *J* = 8.8, 3.4 Hz, 1 H), 5.25 (d, *J* = 12.2 Hz, 2 H), 4.68 (dd, *J* = 8.8, 5.0 Hz, 1 H), 3.97–3.86 (comp, 2 H), 3.66 (s, 3 H), 3.56–3.49 (m, 1 H), 3.21–3.13 (m, 1 H), 2.15–2.02 (m, 1 H), 1.92–1.76 (comp, 2 H), 1.69–1.57 (m, 1 H); ¹³C NMR (75 MHz, CDCl₃) δ 172.1, 168.9, 150.4, 149.3, 137.9, 134.5, 132.7, 129.1, 128.7, 128.6, 128.4, 127.4, 69.0, 60.8, 53.3, 52.8, 48.7, 42.3, 31.0, 24.2. [α]_D²⁴ = -118.4(6) (*c* = 1.0, CH₂Cl₂).

Methyl 1-[1-benzenesulfonyl-pyrrolidine-2'(R)-carboxyl]-3-benzoyloxycarbonyl-2-oxo-imidazolidine-4(S)-carboxylate (S,R-13) was prepared by the same procedure as that described for **S,S-13** (0.96 g, 1.9 mmol, 70% yield). ¹H NMR (300 MHz, CDCl₃) δ 7.91–7.86 (comp, 2 H), 7.63–7.49 (comp, 3 H), 7.39 (br s, 5 H), 5.59 (dd, *J* = 9.1, 3.1 Hz, 1 H), 5.40 (d, *J* = 12.2 Hz, 1 H), 5.25 (d, *J* = 12.2 Hz, 1 H), 4.76 (dd, *J* = 10.2, 3.7 Hz, 1 H), 4.09 (dd, *J* = 12.0, 10.2 Hz, 1 H), 3.85 (dd, *J* = 12.0, 3.7 Hz, 1 H), 3.70 (s, 3 H), 3.63–3.54 (m, 1 H), 3.27–3.17 (m, 1 H), 2.21–2.07 (m, 1 H), 1.97–1.85 (comp, 2 H), 1.78–1.64 (m, 1 H); ¹³C NMR (75 MHz, CDCl₃) δ 172.2, 169.5, 150.2, 149.1, 138.0, 134.5, 132.7, 129.1, 128.7, 128.6, 128.3, 127.4, 69.0, 60.7, 53.1, 52.6, 48.6, 42.3, 31.1, 24.3.

Methyl 1-[1-Benzenesulfonyl-pyrrolidine-2'(S)-carboxyl]-2-oxo-imidazolidine-4(S)-carboxylate, (4S,2'S)-HB-SPIM (S,S-14). A mixture of **S-13** (1.50 g, 2.91 mmol), palladium black (10 mg, 0.094 mmol), and methanol (15 mL) was stirred under a balloon pressure of hydrogen for 2 h. After TLC analysis showed complete conversion to **S-14**, the reaction mixture was filtered through Celite. The resulting solution was concentrated under reduced pressure to a white solid, which was purified by column chromatography (ethyl acetate) to afford 0.94 g of **S-14** (2.467 mmol, 85% yield). ¹H NMR (300 MHz, CDCl₃) δ 7.92–7.87 (comp, 2 H), 7.62–7.49 (comp, 3 H), 5.72 (s, 1 H), 5.60 (dd, *J* = 8.7, 3.7 Hz, 1 H), 4.34 (dd, *J* = 10.3, 4.9 Hz, 1 H), 4.24–4.10 (comp, 2 H), 3.86 (s, 3 H), 3.59–3.57 (m, 1 H), 3.32–3.23 (m, 1 H), 2.17–2.05 (m, 1 H), 2.01–1.84 (comp, 2 H), 1.77–1.65 (m, 1 H); ¹³C NMR (75 MHz, CDCl₃) δ 172.0, 170.3, 154.8, 138.2, 132.7, 129.0, 127.5, 60.0, 53.2, 49.8, 48.7, 45.0, 31.2, 24.4. [α]_D²⁰ = -100.5(4) (*c* 0.93, CH₂Cl₂).

(33) Sheldrick, G. M. *SHELXTL/PC*, version 5.03; Siemens Analytical X-ray Instruments, Inc.: Madison, WI, 1994.

(34) Sheldrick, G. M. *SADABS Siemens Area Detector Absorption Correction*; Universität Göttingen: Göttingen, Germany, 1996.

(35) Sheldrick, G. M. *SHELXTL/PC*, version 6.10; Bruker AXS, Inc.: Madison, WI, 1997.

Methyl 1-[1-benzenesulfonyl-pyrrolidine-2'(R)-carbonyl]-2-oxo-imidazolidine-4(S)-carboxylate, (4S,2'R)-HB-SPIM (S,R-14), was prepared by the same procedure as that described for the preparation of **S-14** (0.763 g, 2.01 mmol, 83% yield). ^1H NMR (300 MHz, CDCl_3) δ 7.94–7.86 (comp, 2 H), 7.63–7.49 (comp, 3 H), 5.71 (s, 1 H), 5.66–5.62 (m, 1 H), 4.39 (dd, $J = 10.5, 4.9$ Hz, 1 H), 4.26 (dd, $J = 11.7, 10.5$ Hz, 1 H), 4.07 (dd, $J = 11.7, 4.9$ Hz, 1 H), 3.82 (s, 3 H), 3.62–3.54 (m, 1 H), 3.31–3.21 (m, 1 H), 2.14–2.02 (m, 1 H), 2.02–1.84 (comp, 2 H), 1.76–1.64 (m, 1 H); ^{13}C NMR (75 MHz, CDCl_3) δ 172.1, 170.6, 154.8, 138.1, 132.7, 129.0, 127.5, 59.7, 53.1, 49.8, 48.7, 45.0, 31.2, 24.5.

Dirhodium(II) Tetrakis{methyl 1-[1-benzenesulfonyl-pyrrolidine-2'(S)-carbonyl]-2-oxo-imidazolidine-4(S)-carboxylate}, (cis-2,2)-[Rh₂(4S,2'S-BSPIM)₄(CH₃OH)₂] (15). A solution of compound **S-14** (0.720 g, 1.9 mmol) and Rh₂(OAc)₄ (0.105 g, 0.24 mmol) in 10 mL of anhydrous chlorobenzene was heated at reflux for 6 h, with rapid flushing (1 flush/min) through a Soxhlet extractor containing a thimble filled with a mixture of 2:1 sodium carbonate/sand. The progress of the ligand exchange reaction was monitored by HPLC using a 3.9 mm \times 150 mm reverse-phase μ -Bondapak-CN column. When conversion to **15** was complete (by HPLC), the solvent was removed under reduced pressure, and the purple solid was purified by passing through reverse phase Bakerbond CN resin (methanol/acetonitrile 99:1) to yield 0.21 g of a purple solid (0.12 mmol, 52% yield): ^1H NMR (300 MHz, CDCl_3) δ 8.09–8.00 (comp, 4 H), 7.83 (d, $J = 11$ Hz, 4 H), 7.59–7.42 (comp, 12 H), 5.58–5.37 (comp, 4 H), 4.22–3.80 (comp, 6 H), 3.78–3.67 (comp, 4 H), 3.85 (s, 6 H), 3.80 (s, 6 H), 3.44–3.30 (comp, 6 H), 2.21–2.07 (comp, 6 H), 1.98–1.86 (comp, 8 H), 1.83–1.63 (comp, 8 H), 0.85–0.82 (comp, 4 H); ^{13}C NMR (75 MHz, CDCl_3) δ 174.4, 173.6, 170.1, 170.0, 164.6, 163.0, 139.0, 138.8, 132.5, 132.3, 128.6, 129.1, 127.0, 58.9, 57.5, 57.0, 52.5, 52.6, 48.8, 48.0, 47.2, 45.0, 31.5, 31.1, 24.1, 24.0, 23.7, 23.6. $[\alpha]^{25}_{\text{D}} = -240(2)$ (c 0.06, CH_2Cl_2). HRMS for $(\text{C}_{64}\text{H}_{72}\text{N}_{12}\text{O}_{24}\text{Rh}_2\text{S}_4)^+$ theoretical 1726.1775 $[\text{M}]^+$; found 1726.1085. Anal. Calcd for Rh₂C₆₄H₈₀N₁₂O₂₈S₄ (containing 2 molecules of water as axial ligands and 2 unassociated water molecules): C, 42.72; H, 4.48; N, 9.34. Found: C, 42.84; H, 4.51; N, 8.90.

X-ray Structure of 15. Crystals grew as red blocks from dry methanol/dichloromethane/acetonitrile (90:9:1). The data crystal had approximately orthogonal dimensions 0.46 \times 0.39 \times 0.25 mm³. Crystals of **15** (Rh₂C₇₁H₈₀N₁₂O₃₂S₄, containing 2 molecules of methanol coordinated in the axial sites) were orthorhombic, space group $P2(1)2(1)2(1)$, with $a = 15.934(3)$, $b = 22.317(5)$, $c = 24.695(5)$ Å, $V = 8782(3)$ Å³, $Z = 4$, $\rho(\text{calc}) = 1.473$ Mg m⁻³. The unit cell contained 5 additional molecules of methanol and 1 molecule of water. Data were collected out to $2\theta = 60^\circ$ by the ω -scan technique at 20 °C using graphite-monochromatized Mo K α radiation ($\lambda = 0.71073$ Å); 89210 reflections were measured of which 18261 were unique [$R_{\text{int}}(F^2) = 0.0867$]. The structure was solved by direct methods and refined by full-matrix least-squares on F^2 with anisotropic displacement parameters for the non-hydrogen atoms. The hydrogen atoms were calculated and placed in idealized positions throughout the refinement and convergence process. The final $R_w(F^2) = 0.1846$ with a goodness of fit = 1.059 for refining 958 parameters. The conventional $R(F) = 0.0705$ for 6955 reflections for $F_o > 3\sigma(F_o)$. Data reduction, decay correction, structure solution, and refinement were done using the SHELXTL/PC software package.³³ An absorption correction was applied with the SADABS program.³⁴ Tables of positional and thermal parameters, bond lengths and angles, and torsion angles and figures are located in a CIF file as Supporting Information.

Dirhodium(II) Tetrakis{methyl 1-[1-benzenesulfonyl-pyrrolidine-2'(R)-carbonyl]-2-oxo-imidazolidine-4(S)-carboxylate}, (cis-2,2)-[Rh₂(4S,2'R-BSPIM)₄(CH₃CN)(PhCN)] (16). Purple crystals of **16** were prepared analogously to the procedure described for compound **15** (0.23 g, 0.13 mmol, 61% yield): ^1H NMR (300 MHz, CDCl_3) δ 7.86–7.79 (comp, 8 H), 7.55–7.44 (comp, 12 H), 6.00–5.94 (comp, 4 H), 4.75 (br dd, $J = 10.1, 5.6$ Hz, 2 H), 4.42–4.35 (comp, 2 H), 4.16 (br t, $J = 11.7$ Hz, 2 H), 3.85 (br s, 6 H), 3.80–3.64 (comp, 6 H), 3.73 (br s, 6 H), 3.56–3.45 (comp, 4 H), 3.34–3.23 (comp, 4 H), 2.26–2.07 (comp, 4 H), 2.15 (s, 6 H), 1.98–1.86 (comp, 4 H), 1.83–1.63 (comp, 4 H), 1.59–1.47 (comp, 2 H), 1.33–1.22 (comp, 2 H); ^{13}C NMR (75 MHz, CDCl_3) δ 174.7, 173.3, 170.0, 169.9, 164.3, 163.1, 138.8, 138.6, 132.8, 132.6, 128.9, 128.8, 127.3, 58.6, 57.6, 57.0, 52.5, 52.6, 48.6, 48.0, 47.0, 46.3, 31.8, 30.9, 24.4, 24.3, 23.9, 23.8. $[\alpha]^{25}_{\text{D}} = -97.1$ (c 0.068, CH_2Cl_2). HRMS for $(\text{C}_{64}\text{H}_{73}\text{N}_{12}\text{O}_{24}\text{Rh}_2\text{S}_4)^+$ theoretical 1727.1848 $[\text{M} + \text{H}]^+$; found 1727.0175. Anal. Calcd for Rh₂C₆₄H₈₀N₁₂O₂₈S₄ (containing 2 molecules of water as axial ligands and 2 unassociated water molecules): C, 42.72; H, 4.48; N, 9.34. Found: C, 42.84; H, 4.18; N, 9.55.

X-ray Structure of 16. Crystals grew as red blocks from dry methanol/benzonitrile/acetonitrile (96:3:1). The data crystal had approximately orthogonal dimensions 0.28 \times 0.23 \times 0.16 mm³. Crystals of **16** contained two dirhodium molecules in the asymmetric unit (Rh₂C_{151.50}H₁₆₄N₂₈O_{48.50}S₈, each dirhodium core containing one molecule of acetonitrile and one molecule of benzonitrile coordinated in the axial sites). Crystals were triclinic, space group $P1$, with $a = 14.4850(9)$, $b = 15.0017(9)$, $c = 20.5200(12)$ Å, $V = 4121.0(4)$ Å³, $Z = 1$, $\rho(\text{calc}) = 1.540$ Mg m⁻³. The unit cell additionally contained half a molecule of methanol. Data were collected out to $2\theta = 55.11^\circ$ by the ω -scan technique at -100 °C using graphite-monochromatized Mo K α radiation ($\lambda = 0.71073$ Å); 65840 reflections were measured of which 37331 were unique [$R_{\text{int}}(F^2) = 0.0338$]. The structure was solved by direct methods and refined by full-matrix least-squares on F^2 with anisotropic displacement parameters for the non-hydrogen atoms. The hydrogen atoms were calculated and placed in idealized positions throughout the refinement and convergence process. The final $R_w(F^2) = 0.1221$ with a goodness of fit = 1.054 for refining 2105 parameters. The conventional $R(F) = 0.0496$ for 30413 reflections for $F_o > 2\sigma(F_o)$. Data reduction, decay correction, structure solution, and refinement were done using the SHELXTL/PC software package.³³ An absorption correction was applied with the SADABS program.³⁴ Tables of positional and thermal parameters, bond lengths and angles, and torsion angles and figures are located in a CIF file as Supporting Information.

Acknowledgment. The National Institutes of Health (GM 46503) and the National Science Foundation (CHE9610374, X-ray diffractometer) supported this work. The authors thank Dr. Christopher Welch (Merck, Inc.) for his generous donation of chromatographically separated *trans*-2-phenylcyclopropanecarboxylic acid enantiomers.

Supporting Information Available: Additional experimental details, ^1H and ^{13}C NMR spectra, tables of positional and thermal parameters, and X-ray crystallographic information in CIF format. This material is available free of charge via the Internet at <http://pubs.acs.org>.

JO0506090